A Novel Segmented Electrode Schematic for Pulsed Plasma Thrusters

IEPC-2017-319

Presented at the 35th International Electric Propulsion Conference
Georgia Institute of Technology • Atlanta, Georgia • USA
October 8 – 12, 2017

Zhe Zhang[1], Haibin Tang[2],
Beihang University, Beijing, 100191, China
William Yeong Liang Ling[3]
Beijing Institute of Technology, Beijing, 100191, China
Junxue Ren[4]
Beihang University, Beijing, 100191, China
Thomas M. York[5]
Professor Emeritus, Ohio State University, Columbus, Ohio 43235, USA

Abstract: We propose a unique design with "segmented anode" for an ablative pulsed plasma thruster (APPT). The anode consists of conducting upstream and downstream segments interrupted by an insulating ceramic segment. The upstream segment is intended to predominantly carry the current in the early discharge, and the downstream segment is electrically connected to the upstream anode to maintain the downstream electric field in the later discharge. This paper reports on the improvements that this new electrode configuration creates on the performance of a standard APPT. Impulse bit, mass shot and magnetic field strength of the discharge arc were evaluated using a thrust stand, an electronic balance and a magnetic probe. Data indicate that the segmented anode APPT shows an improvement in the impulse bit of up to 28%. The thrust efficiency is also improved from 5.3% to 7.9% for the conventional and segmented designs, respectively. The magnetic probe data show a more intense arc current density on the segmented anode PTFE surface than on that of the standard anode PPT. These results are indicative of a fundamental change in the physical mechanisms behind an increased performance of an APPT with a segmented anode. This improvement results from changes that are both simple and effective and can be easily applied on other APPT designs.

I. Introduction

ELECTRIC propulsion systems are plasma sources with the advantage of a high efficiency making them popular for spacecraft orbital control[1]. Pulsed plasma thrusters are a type of electric thruster with precise thrust levels and low power requirements[2, 3], making them suitable for small satellites such as CubeSats[4]. APPTs have system advantages such as reliability, low cost, high specific impulse, and compact systems compared to conventional chemical thruster; the compact system and precise thrust control make it a competitive spacecraft thruster[5, 6].

[1] PhD student, Mr, Beihang University, zhangzheplasma@buaa.edu.cn
[2] Professor, PhD, Beihang University, thb@buaa.edu.cn
[3] Associate Professor, PhD, Beijing Institute of Technology, wling@bit.edu.cn
[4] Associate Professor, PhD, Beihang University, rjx_buaa@163.com
[5] Professor Emeritus, PhD, Ohio State University, tmy1215@aol.com

However, the efficiency level and μN-level thrust are detriments and caused the PPT to be abandoned for alternative thrusters.

The operating mechanisms of the APPT involve physical processes such as material ablation[7,8], ionization[9], vacuum arc discharges[10], and electromagnetic acceleration[11,12], thus requiring a wide field of theoretical and experimental understanding. Also the APPTs' several microsecond duration discharge and the related electromagnetic interference from the main discharge make measurements difficult. These challenges have resulted in the lack of thorough understanding of the physical processes occurring in the APPT. Despite a relatively long research history, low efficiency is still is the key issue to be addressed to improve the APPTs performance.

In the past several years, research has focused on parametric studies to optimize electrode designs to determine the flare angle, width and electrode spacing that produces the best performance for a given PPT[13] [14]. However, these studies on electrode design focus on optimization and do not represent a significant foundation for PPT development. The performance of APPTs specifically addressing impulse bit and thrust efficiency need to be further examined to identify mechanisms for further improvement.

This paper evaluates the performance of a new design of a segmented anode APPT. The performance of an APPT with normal anode and one with a segmented anode was studied using data from a magnetic probe, thrust stand, and electronic balance. Using that data, the resulting magnetic field of the discharge arc, impulse bit, and thrust efficiency can be compared for the normal anode and segmented anode APPTs.

II. Experimental apparatus

a. Vacuum system

The PPT experiments were conducted in a vacuum chamber with a diameter of 0.8 m and a length of 1.8 m. The chamber was equipped with a DIS-500 rotary pump and a CRYO-U 12HSP cryogenic pump. A base pressure of 3×10^{-3} Pa was reached before experiments were conducted. The vacuum chamber is shown in Figure 1.

Figure 1. Vacuum chamber.

b. Pulsed plasma thruster with normal and segmented anode configurations

A schematic of the breech-fed experimental APPT with conventional parallel electrodes (called "normal anode" in this paper is shown in Figure 2; this configuration is similar to rectangular geometry APPTs previously studied by Lau et al.[15] and Koizumi et al.[11]. The components consist of five main parts: the anode, cathode, spark plug, propellant (PTFE), and capacitor. The oil capacitor (10 μF) was rated for a maximum voltage of 2000 V; the corresponding discharge energy range was from 0 – 20 J. The electrode length was 20 mm; the gap between the anode and cathode was 20 mm, and the electrode width was 18 mm.

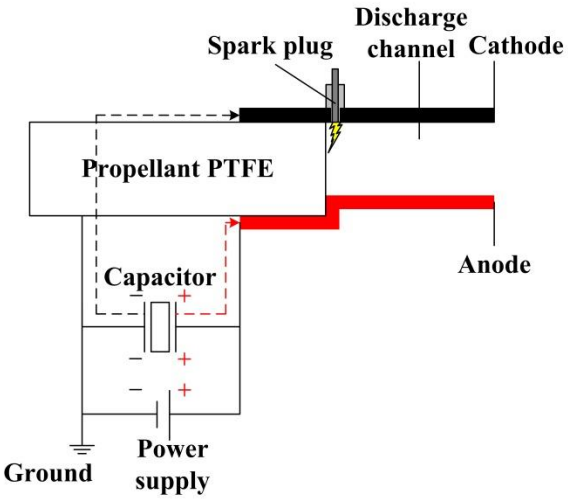

Figure 2. APPT with normal anode schematic.

The downstream anode segment was copper and was insulated from the main copper anode using a ceramic element as shown in Figure 3; this anode arrangement is referred to as a "segmented electrode".

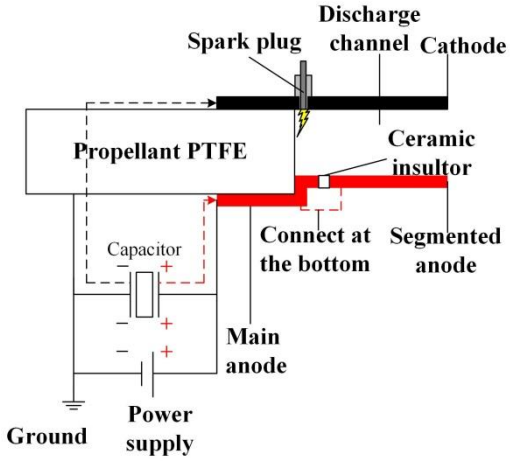

Figure 3. Segmented anode PPT structure.

A common characteristic of the parallel electrode APPT is a diffuse arc along the anode[11]. The more diffuse arc results in a lower current density along the PTFE surface, which not only results in less mass ablation but also less ionization. The new segmented anode configuration was designed to alter discharge phenomena in order to improve PPT performance. It is expected to induce better main discharge characteristics from the shorter upstream anode and maintain the downstream electric field between the electrodes.

c. Thrust stand

In order to measure the impulse bit produced by the APPT with both normal and segmented anode configurations, a thrust stand was utilized. The thrust stand is shown in Figure 4. This torsional thrust stand is of a type similar to that described in Reference16. The thrust stand includes four main parts: a torsional arm, flexural pivots, stationary structure, and displacement sensor. It has a measurement range of 10 – 1000 μN·s. Since the APPT is tested in single-shot mode, the oscillation of thrust stand will follow the torsional harmonic motion. The displacement of the torsional arm is recorded by the displacement sensor and is converted into a voltage signal. Using the measured displacement and the parameters of the thrust stand, the equations of harmonic motion allow estimation of the impulse produced by the PPT. The thrust stand has been successfully used for energy levels of 5, 7.5, 10, 12.5, 15, 17.5, and 20J.

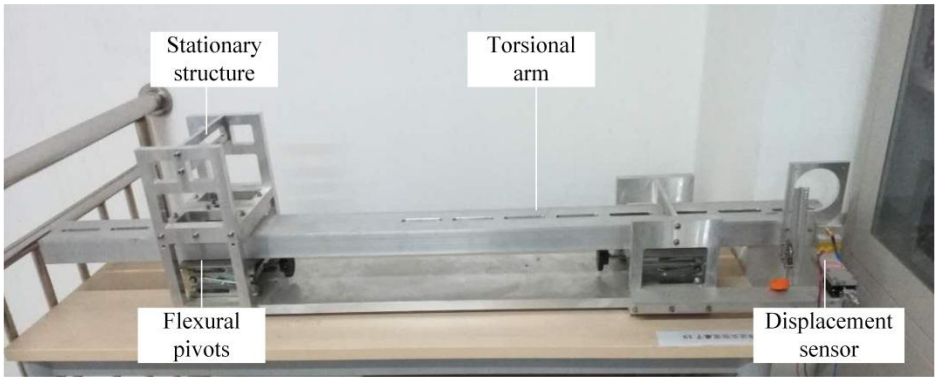

Figure 4. Thrust stand.

d. Electronic balance

During APPT operation, propellant will be ablated and some will be ionized. The mass of consumed propellant can be used to calculate the thrust efficiency. Mass measurements were conducted using an electronic balance (Mettler Toledo XS205) with a resolution of 0.01 mg, a repeatability error of 0.02 mg for masses <10 g, and a range of 0 – 220 g. The electronic balance is shown in Figure 5.

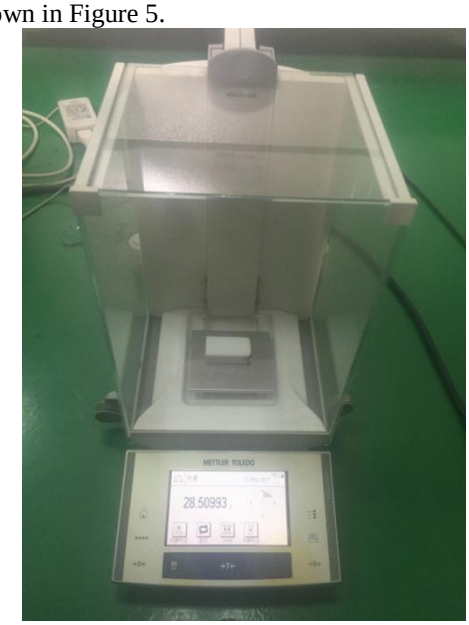

Figure 5. Electronic balance.

Four energy levels were examined in the experiments: 5, 10, 15, and 20 J for both normal and segmented anode configurations. For each energy level, data were collected as averages over the APPT's 500 shots. There were 12 PTFE blocks used for the experiments: 4 energy levels × 3 anode types. Following the discharges, 12 weight measurements were recorded after the vacuum chamber was vented for 1 hour to standardize any errors due to moisture absorption from the atmosphere.

e. Micro-magnetic probe

The twisted loop magnetic probe is a typical means of measuring time-varying magnetic fields[17,18]. In order to study the differences in the PTFE surface discharge characteristics between normal and segmented anode APPTs, a micro-magnetic probe of small size was fabricated so as to produce minimal disturbance in the discharge channel space (Figure 6). The micro-magnetic probe of enamel insulated wire had a diameter of 2 mm, wire diameter of 0.12 mm, and was wound for 40 turns around a core holder with a diameter of 1.8 mm. The entire construct was covered with an epoxy shell. During a single pulse discharge of the PPT, the probe was located inside of the conducting plasma. Calibration was performed using the Biot–Savart law to obtain the local magnetic field strength from

measured current from a Rogowski coil. The probe signal after the RC integration circuit (τ = 48 μs) is proportional to local magnetic field strength.

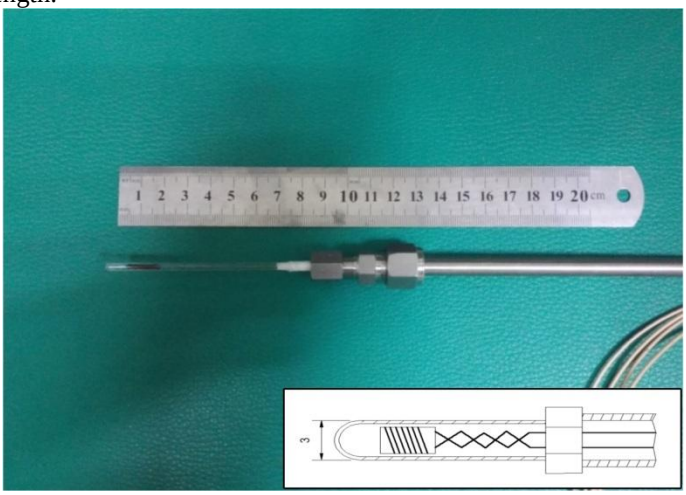

Figure 6. Micro-magnetic probe schematic.

The probe was positioned between the electrodes with measurement points as shown in Figure 7.

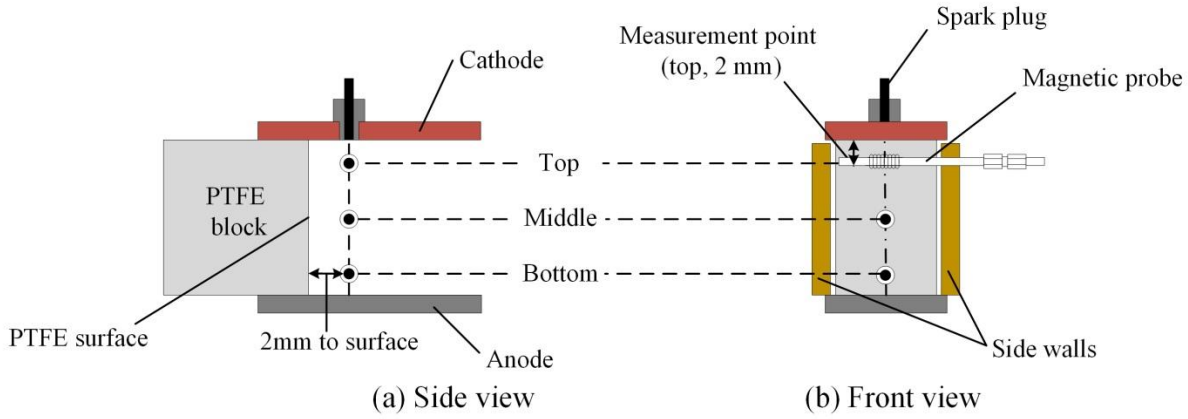

Figure 7. Micro-magnetic probe measurement points.(a) Side view and (b) front view schematics of the APPT inner-electrode area.

Measurements were taken at an axial location 2 mm from the PTFE surface for three vertical positions (top, 2 mm from the cathode; middle, 10 mm from the cathode; bottom, 18 mm from the cathode).

III. Results and discussion

a. Long duration luminosity images for normal and segmented anode configurations

Since the discharge occurs over a time scale of ~10 μs, any exposure time longer than this will capture the entire discharge process in a single image. A Nikon D750 was used to photograph the images for normal and segmented anode configurations. The experiments were conducted at a discharge voltage 2000 V and a discharge energy of 20 J. In Figure 8, the segmented anode configuration can be seen to affect qualitatively the morphology of the discharge arc on the propellant surface (polytetrafluoroethylene, i.e., PTFE). The electrical connection between the upstream and downstream anode segments would maintain a downstream electric field between cathode and anode, similar to the normal anode.

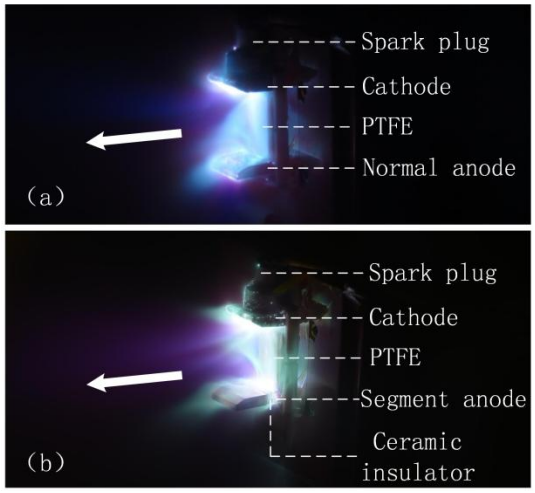

Figure 8. Long-duration exposure images of the plasma morphology for a (a) normal, and (b) segmented anode PPT.

In Figure 8, there are evident differences in the luminosity distribution and the plasma morphology. The areas near the electrodes are distinctly different for the normal anode as compared to the segmented anode. The luminosity distributions along the anodes (the bottom) show that on a normal PPT, the discharge arc may possibly travel farther downstream while the segmented anode PPT arc is isolated extremely close to the PTFE surface. From the qualitative plasma morphology, the discharge from a PPT with a segmented electrode appears to be sharper and more parallel with the electrodes than that of a normal PPT.

The downstream plasma morphology along the channel and away from the segmented electrodes shows a higher intensity central plasma area. While the segmented anode appeared to have made the current more intense near the PTFE surface, it also seems that the plasma was focused toward the middle of the electrodes. On the normal PPT, the luminosity distribution was even and smooth across the entire anode. On the segmented anode the luminosity patterns was brighter and more intense. The downstream plasma for the normal anode had less collimation compare to segment anode.

The images of plasma morphology, while not quantitative, provide indications of differences in the discharge process of the segmented electrode PPT. For the normal PPT, the arc is wide and smooth. For the segmented anode PPT, the arc is intense and more clearly visible than for the normal PPT, and the plasma in the discharge channel is focused to the middle of the electrode. The presence of an insulator between the segments may impose a limitation to the downstream propagation of the discharge arc, which may result in a higher current intensity on the propellant surface. The arc produced by the segmented anode PPT is straighter and more intense, which is good for the plasma acceleration. All these phenomenological differences require the support of further measurements.

b. Thrust stand measurements

A μN-level thrust stand was used to measure the impulse bits generated by PPTs with normal and segmented anodes over an energy range of 5 – 20 J. Details regarding the thrust stand and impulse bit calculations can be found in Reference 16. The impulse bit evaluation results are shown in Figure 9. Every data point for a given energy is the average of 10 shots to ensure repeatability. At an energy of 20J, when all other variables such as the power supply, capacitor, and propellant were the same. the impulse bit of a segmented anode PPT was found to be 28% higher than that of a normal anode PPT. The largest standard deviation occurred at an energy level of 20 J; two standard deviations over all the data points for 20 J with a normal anode APPT was determined to be 9.2 μN·s.

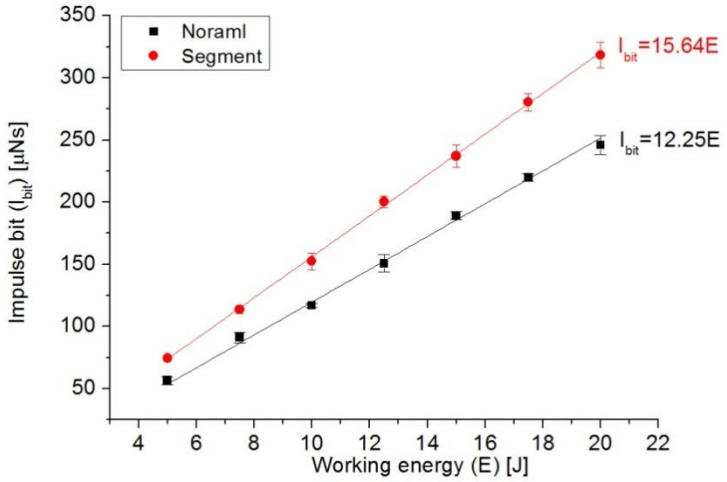

Figure 9. Impulse bits of normal (black)and segmented anode (red) PPT. The error bars indicate the maximum errors of the average values.

As was noted above from the long duration luminosity image results, the segmented anode scheme suggested a higher current intensity on the propellant surface which could result in better performance of APPTs. Figure 9 shows data that indicate impulse bits of segmented anode > normal anode. The increase in impulse bit was consistent across discharge energy levels; the segmented anode demonstrated an impulse bit that was approximately 28% higher than that of the normal anode APPTs. This result is consistent with the idea that while the upstream segment may act to improve the APPT ablation process, the downstream segment still plays a role in further increasing the impulse bit as with a normal anode APPT.

c. Mass shot and thrust efficiency results

In order to evaluate the APPT performance, experimental data on the mass bit are necessary. Each propellant sample block was evaluated under the same vacuum and temperature. After 500 shots for each block, the ablation surfaces are presented in Figure 10 for comparison.

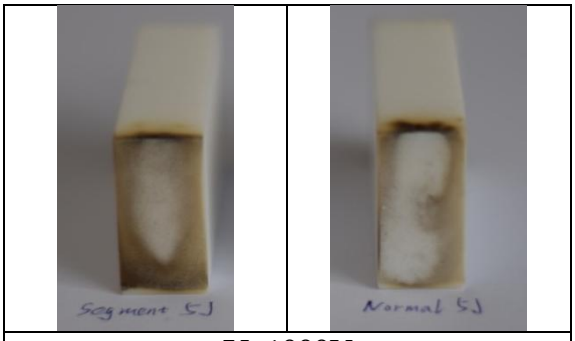

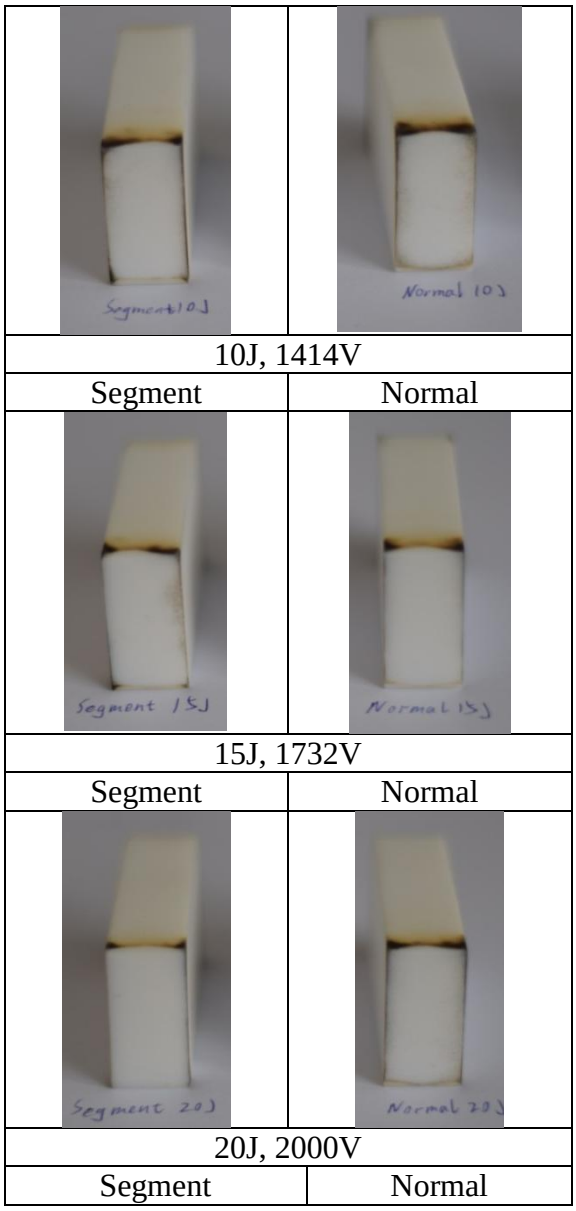

Figure 10. Ablation surfaces for normal and segmented anode APPTs

The total weight measurement error after 500 shots was on the order of 0.1mg. The mass shot data for the normal and segmented anode APPTs are shown in Table 2. Using the mass shot and impulse bit data, the APPTs performance parameters such as mass bit per shot ∆ m, specific impulse (I_{sp}), thrust efficiency (η_t), mass bit per joule ($\Delta m/E$) were calculated.

The specific impulse (I_{sp}) of the thruster is:

$$I_{sp} = \frac{I_{bit}}{\Delta m g}, \tag{1}$$

where g is gravitational acceleration. The thrust efficiency (η_t) can be calculated using:

$$\eta_t = \frac{I_{bit}^2}{2\Delta m E}, \tag{2}$$

where E is the discharge energy.

Thruster parameters including Δm, I_{sp},η_t, $\Delta m/E$ are presented in Table 1 for the APPT with normal and segmented anodes at different energy levels. The values are typical for an APPT[2,19].

Table 1. Comparison of APPT performance with different anodes.

Thruster type	Energy level $E(J)$	Specific impulse, $I_{sp}(s)$	Impulse bit I_{bit} $(\mu N{\cdot}s)$	Mass bit per shot $\Delta m(\mu g)$	$\Delta m/E$, $(\mu g/J)$	Thrust efficiency, η_t (%)
Normal	20	856	246	28.74	1.44	5.3
Segment	20	997	318	31.88	1.59	7.9
Normal	15	886	189	21.32	1.42	5.6
Segment	15	997	237	23.78	1.59	7.9
Normal	10	816	117	14.34	1.43	4.8
Segment	10	887	152	17.14	1.71	6.7
Normal	5	747	56	7.5	1.5	4.2
Segment	5	808	74	9.16	1.83	6.0

First, as can be seen in Figure 10, at various energies the carbon deposition for normal and segmented anode APPTs appears different. At low energy (5J), the segmented anode PPT has a more serious carbon deposition than that of normal anode PPT. However, at high energy (20 J), the segmented anode PPT has a much cleaner surface than that of normal anode PPT. This behavior has some correlation with results presented in Table 1; the efficiency for the segmented anode PPT increased by 1.8% at 5 J, while the efficiency for segmented anode PPT increased by 2.6% at 20 J. This result is indicative that a segmented anode APPT has better performance compared to the normal APPT at the same energy level, and this improvement increases with energy.

From Table 1, it can be seen that the segmented anode results in a higher ablated mass than the normal anode APPT. This agrees well with the long duration images and our design assumption that a segmented anode would result in a greater discharge arc current density on the PTFE surface. Importantly, Table 1 also shows that the segmented anode configuration results in both greater impulse bit and thrust efficiency at all the examined energy levels when compared with normal anode APPT.

d. Magnetic probe results

Local measurements of magnetic field were made in the discharge channel in order to clarify the global measurements of thruster performance reported above. Peak values of the probe signal dB/dt are directly related by Faraday law [18], to the local current density of the nearby discharge arc. For a discharge voltage of 1800 V (16.2 J) measurements were taken at a 2mm axial location (Fig. 10) and are presented for different vertical positions in Table 2. Every measurement point has data averages from 10 shots.

Table 2.Peak values of the probe signal for normal and segmented anode APPTs

	Position	dB/dt peak values (V)	Error (±V)
Normal	Top	97	-32 to 39
	Middle	183	-20 to 15
	Bottom	251	-46 to 39
Segment	Top	198	-48 to 40
	Middle	273	-40 to 20
	Bottom	258	-47 to 33

With the (dB/dt) results as representative of the local current density at surface arc, the normal and segmented anode configurations can be concluded to exhibit different discharge characteristics near the PTFE surface. For the normal anode, the dB/dt is lower at the top compared to the bottom. However, for the segmented anode, the dB/dt at the top (near the anode) is much higher than that of a normal PPT while it is slightly higher at other areas. The data suggest that a shorter upstream segment may result in a greater current density in the discharge arc, which will result in better ionization and greater mass ablation. In both configurations, the downstream electric field would still be maintained to enhance plasma containment. These results correlate well with the impulse bit and mass bit results discussed above.

IV. Conclusion

The examination of segmented anode performance reported here represents a new direction in PPT research. The segmented anode APPT configuration applied here shows an improvement in the impulse bit of up to 28% compared to that with conventional symmetric parallel electrodes. The thrust efficiency was also improved by 49% (from 5.3% to 7.9% for conventional and segmented designs, respectively). This improvement in the impulse bit and discharge performance with the use of a segmented anode, while significant, was easily applied to an existing PPT design. However, further work is still necessary to identify the physical mechanisms behind the detailed operation of a PPT with a segmented electrode. The present data suggest that a segmented anode improves impulse bit, thrust efficiency, surface arc intensity and positively alters the discharge arc morphology. However, further experiments will be needed to further understand and develop this new scheme both experimentally and theoretically. In particular, further measurements with Langmuir probe and high speed camera data gathering are planned in future experiments.

The segmented design can be easily implemented and tested on almost all parallel-plate PPTs. The effective application of a practical PPT requires the optimization of several design variables such as the electrode spacing, length, shape, etc. to obtain the desired thruster specifications. The segmented electrode appears to be another avenue for optimization in the future. Design variables such as the insulating segment length and the upstream-to-downstream segment length ratio can also be studied to determine the effect they have on the performance of a thruster.

References

[1] Schönherr T., Encyclopedia of Plasma Technology, edited by Shohet, J. (Taylor & Francis, New York, 2016) 2, 1452-1461.

[2] Burton R. L. and Turchi P. J., "Pulsed Plasma Thruster", Journal of Propulsion and Power, 14(5),716-735, 1998.

[3] Kazeev M. N., Kozubskiy K. N., Popov G. A., "Victor Khrabrov – Pioneer of the First Space ElectricPropulsion System Development and Space Tests", 31st IEPC, IEPC-2009-235, Michigan, 2009.

[4] Panetta P. V., Culver H., Gagosian J., et al. "NASA-GSFC Nano-satellite technology development", 1998.

[5] Mazouffre S., Plasma Sources Science & Technology, 25(3), 033002, 2016.

[6] Jahn R. G., in Physics of Electric Propulsion,(McGraw-Hill, New York,1968), Chap. 9.

[7] Alexeev Y. A., Kazeev M. N., "Performance Study of High Power Ablative Pulsed Plasma Thruster", IEPC-99-207, 1999.

[8] Yang L., Liu X., Wu Z., Applied Physics Letters, 104(8), 084102-084102-4, 2014.

[9] Schönherr T., Nees F., Arakawa Y., Komurasaki K., Herdrich G., Physics of Plasmas, 20(3), 033503(1-8), 2013.

[10] Keidar M., Boyd I. D., Beilis I. I., Journal of Physics D Applied Physics, 34(11), 115-127,2001.

[11] Koizumi H., Noji R., Komurasaki K., Arakawa Y., Physics of Plasmas, 14(3), 033506-033506-10, 2007.

[12] Schönherr T., Komurasaki K., Herdrich G., World Academy of Science, Engineering and Technology, 563-569, 2011.

[13] Schönherr T., Nawaz A., Herdrich G., Röser H. P., and Auweter-Kurtz M., Journal of Propulsion and Power, 25, 380 (2009).

[14] Palumbo D. J., Guman W. J., Journal of Spacecraft & Rockets.13(3), 896467-896467,1976.

[15] Nawaz A., Lau M., Herdrich G., et al. "Investigation of the Magnetic Field in a Pulsed Plasma Thruster", Aiaa Journal, 46(11), 2881-2889, 2012.

[16] Tang H. B., Shi C. B., Zhang X. A., Zhang Z., Cheng J., Review of Scientific Instruments, 82(3), 035118,2011.

[17] Markusic T. E., Current sheet canting in pulsed electromagnetic accelerators, PhD thesis, Princeton University, 2002.

[18] Lau M., Herdrich G., Vacuum, 110(110), 165-171, 2014.

[19] Rezaeiha A., Schönherr T., Journal of Propulsion and Power, 30(2), 253-264, 2015.